The Application of Catastrophe Theory to Image Analysis

A. Kuijper [a,*], L.M.J. Florack [b]

[a] *Utrecht University, Institute of Information and Computing Sciences, Padualaan 14, NL-3584 CH Utrecht, The Netherlands*

[b] *Technical University Eindhoven, Department of Biomedical Engineering, Den Dolech 2, NL-5600 MB Eindhoven, The Netherlands*

Abstract

In order to investigate the deep structure of Gaussian scale space images, one needs to understand the behaviour of critical points under the influence of blurring. We show how the mathematical framework of catastrophe theory can be used to describe the various different types of annihilations and the creation of pairs of critical points and how this knowledge can be exploited in a scale space hierarchy tree for the purpose of pre-segmentation. We clarify the theory with an artificial image and a simulated MR image.

Key words:
scale space, catastrophe theory, critical points, topology, deep structure, multi-scale segmentation.

1 Introduction

The presence of structures of various sizes in an image demands almost automatically a collection of image analysis tools that is capable of dealing with multiple scales simultaneously. Various types of multi-scale paradigms have been developed [60]. They can be divided into two groups: linear and non-linear scale spaces.

* Corresponding author.
Email addresses: arjan@cs.uu.nl (A. Kuijper), L.M.J.Florack@tue.nl (L.M.J. Florack).

The Application of Catastrophe Theory to Image Analysis

A. Kuijper and L.M.J. Florack

UU-CS-2001-23 TR
September 2001

1.1 Scale space

The concept of (linear) scale space has been introduced in the Western world by Witkin [69] and Koenderink [40]. They showed that the natural way to represent an image at finite resolution is by convolving it with a Gaussian of various bandwidths, thus obtaining a smoothened image at a scale determined by the bandwidth. This approach has lead to the formulation of various invariant expressions – expressions that are independent of the coordinates – that capture certain features in an image at distinct levels of scale [13,14,19–23].

Under convolution with a Gaussian features are blurred and their locations change as a function of scale, as long as they remain well-defined. To avoid this a much as possible, non-linear scale spaces have been introduced, in which *e.g.* the blurring on parts with a high gradient (i.e. edges) is much smaller than in the rest of the image [18,58,68].

Multi-scale approaches are nowadays becoming more and more common and are being integrated with methods using PDEs, variational approaches and mathematical morphology [1,8,15,17,29,30,32,53,54].

1.2 Deep Structure

In this paper we focus on linear, or Gaussian, scale space. This has the advantage that each scale level only requires the choice of an appropriate scale; and that the image intensity at that level follows linearly from any previous level. It is therefore possible to trace the evolution of certain image entities over scale. The exploitation of various scales simultaneously has been referred to as *deep structure* by Koenderink [40]. It pertains to information of the change of the image from highly detailed – including noise – to highly smoothened. Furthermore, it may be expected that large structures "live" longer than small structures (a reason that Gaussian blur is used to suppress noise). The image together with its blurred version was called "primal sketch" by Lindeberg [48–50]. Since multi-scale information can be ordered, one obtains a hierarchy representing the subsequent simplification of the image with increasing scale. In one dimensional images this has been done by several authors [33,35,36,67], but higher dimensional images are more complicated as we will discuss below.

1.3 Related Work

An essentially unsolved problem in the investigation of deep structure is how to establish meaningful links across scales. This linking can be region-wise, that

is: all points that belong to a certain region are identified with that region and are connected to a similar region at a larger scale, *cf.* multi-scale watershed segmentation [25,32,55–57]. A disadvantage is that one firstly needs to define these regions.

Another way is to link points if they satisfy some constraint. Vincken *et al.* [42,65,66] built the so-called *hyperstack*, based on a linear scale space, but with linking essentially based on the "affection" between two potentially corresponding points. It appeared that this line of approach also worked well if non-linear scale spaces were used. A drawback of the hyperstack is the counter-intuitively linking in a fine-to-coarse direction.

A well-defined and user-independent strategy is obtained by linking points that satisfy a topological constraint. This approach has been used in 2-D images by various authors [28,47,61]. They linked extrema, but noticed that sometimes new extrema occurred, disrupting a good linking.

This creation of new extrema in scale space has been studied in detail by Damon [10–12], proving that these creations are generic in images of dimension larger than one. That means that they are not some kind of artifact, introduced by noise or numerical errors, but that they are to be expected in any typical case. This was somewhat counterintuitive, since blurring seemed to imply that structure could only disappear, thus suggesting that only annihilations could occur. Damon, however, showed that both annihilations and creations are generic catastrophes. Whereas Damons results were stated theoretically, application of these results were reported in *e.g.* [27,43,47,48].

The main consequence is that in order to be able to use the topological approach one necessarily needs to take into account these creation events. This has been done in previous work by Kuijper *et al.* [44–46].

Apart from the aforementioned catastrophe points (annihilations and creations) there is a second type of topologically interesting points in scale space, *viz.* scale space critical points. These are spatial critical points with vanishing scale derivative. This implies a zero Laplacean in linear scale space. Although Laplacean zero-crossings are widely investigated (the "Laplacean of Gaussian" as edge-detector), the combination with zero gradient has only been mentioned occasionally, *e.g.* by [27,41,47].

Several authors investigated the shape of iso-intensity manifolds [27,31,40] in scale space. Obviously, at annihilations some structure disappears. However, these points are not the only special points in relation to the iso-intensity manifolds as we showed in [44]. In contrast, in [44] we proved that the *critical points in scale space* also form special points as these define so-called *critical iso-intensity manifolds*, *i.e.* iso-intensity manifolds with self-intersection encapsulating an extremum, see Section 2.4.

Scale space critical points, together with annihilations and creations allow us to build a hierarchical structure that can be used to obtain a so-called pre-segmentation: a partitioning of the image in which the nesting of iso-intensity manifolds becomes visible.

1.4 Aim

In the aforementioned articles [44–46] we also showed that it is sometimes desirable to use higher order (and thus non-generic) catastrophes to describe the change of structure. It has a direct relation to the hierarchy tree and the pre-segmentation, in the sense that two or more regions can be endowed with the same critical iso-intensity manifold. In this paper we describe these catastrophes in scale space and show the implications for both the hierarchy tree and the pre-segmentation.

In section 2 theory on Gaussian scale space, catastrophe theory and a brief outline of the hierarchy tree is given. Catastrophes in scale space in generic coordinates and their effects on the hierarchy are discussed in section 3. We give some applications in section 4 and end with a summary and discussion in section 5.

2 Theory

In [44] we presented a uniquely defined hierarchical structure describing a scale space image. In section 2.4 we shortly outline the basic steps. In order to understand the essential elements, we define a Gaussian scale space in section 2.1. The structure depends on the evolution of spatial critical points as the scale changes. The locations of these points in scale space form one dimensional manifolds, the so-called critical curves, containing two types of special points. The first type is formed by the scale space saddles, discussed in section 2.2. The second type are the catastrophe points, presented in section 2.3.

2.1 Gaussian Scale Space

Definition 1 $L(\mathbf{x})$ *denotes an arbitrary n-dimensional image. We will refer to this image as the* initial image*.*

Definition 2 $L(\mathbf{x};t)$ *denotes the* $(n+1)$*-dimensional* Gaussian scale space image *of* $L(\mathbf{x})$*.*

The Gaussian scale space image is obtained by convolution of an initial image with a normalised Gaussian kernel of zero mean and standard deviation $\sqrt{2t}$:

$$L(\mathbf{x};t) = G(\mathbf{x};t) \otimes L(\mathbf{x}) = \int \frac{1}{\sqrt{4\pi t}^n} \, e^{-\frac{|\mathbf{x}-\mathbf{y}|^2}{4t}} L(\mathbf{y}) \, d\mathbf{y} \ .$$

Consequently, $L(\mathbf{x};t)$ satisfies the diffusion equation:

$$\partial_t L(\mathbf{x};t) = \sum_{i=1}^{n} \frac{\partial^2}{\partial x_i^2} L(\mathbf{x};t) \stackrel{\text{def}}{=} \Delta L(\mathbf{x};t) \ . \tag{1}$$

Here $\Delta L(\mathbf{x};t)$ denotes the Laplacean. Differentiation is now well-defined, since derivatives of the image up to arbitrary order at any scale are given by

$$\frac{\partial}{\partial x_i} L(\mathbf{x};t) = \frac{\partial}{\partial x_i} \left(G(\mathbf{x};t) \otimes L(\mathbf{x}) \right) = \left(\frac{\partial}{\partial x_i} G(\mathbf{x};t) \right) \otimes L(\mathbf{x}).$$

That is, an arbitrary derivative of the image is obtained by the convolution of the initial image with the corresponding derivative of a Gaussian.

Definition 3 *Spatial critical points, i.e. saddles and extrema (maxima or minima), at a certain scale t_0 are defined as the points at fixed scale t_0 where the spatial gradient vanishes: $\frac{\partial}{\partial_{x_i}} L(\mathbf{x};t_0) = 0 \ \forall i$, that is, $\nabla L(\mathbf{x};t_0) = 0$. We will refer to these points as* spatial critical points *to distinguish them from scale space critical points, see Definition 6.*

The type of a spatial critical point is given by the eigenvalues of the Hessian H, the matrix with the second order spatial derivatives, evaluated at its location.

Definition 4 *The Hessian matrix at a certain scale t_0 is defined by $H \stackrel{\text{def}}{=} \nabla\nabla^T L(\mathbf{x};t_0)$, where each element of H is given by*

$$H_{i,j} = \frac{\partial^2}{\partial x_i \partial x_j} L(\mathbf{x};t).$$

The trace of the Hessian equals the Laplacean. For maxima (minima) all eigenvalues of the Hessian are negative (positive). At a spatial saddle point H has both negative and positive eigenvalues.

Since $L(\mathbf{x};t)$ is a smooth function in $(\mathbf{x};t)$-space, spatial critical points are part of a one dimensional manifold in scale space by virtue of the implicit function theorem.

Definition 5 *A* critical curve *is a one-dimensional manifold in scale space on which $\nabla L(\mathbf{x};t) = 0$.*

Consequently, the intersection of all critical curves in scale space with a plane of certain fixed scale t_0 yields the spatial critical points of the image at that scale.

2.2 Scale Space Saddles

Definition 6 *The* scale space saddles *of* $L(\mathbf{x};t)$ *are defined as the points where both the spatial gradient and the scale derivative vanish:* $\nabla L(\mathbf{x};t) = 0$ *and* $\Delta L(\mathbf{x};t) = 0$.

In Definition 6 we used Eq. (1). Note that it describes the critical points of $L(\mathbf{x};t)$ in scale space. In [44] it is proven that these points are indeed always saddle points, a result of the well-known maximum principle.

Definition 7 *The* extended Hessian $\mathcal{H}$ *of* $L(\mathbf{x};t)$ *is matrix of second order derivatives in scale space defined by*

$$\mathcal{H} = \begin{pmatrix} \nabla\nabla^T L & \Delta\nabla L \\ (\Delta\nabla L)^T & \Delta\Delta L \end{pmatrix}.$$

Here $\nabla\nabla^T L$ *is the Hessian.*

Note that the elements of $\mathcal{H}$ are purely spatial derivatives. Again, this is possible by virtue of the diffusion equation, Eq. (1).

The fact that scale space critical points are always saddles implies that the extended Hessian has both positive and negative eigenvalues at scale space critical points. Furthermore, in [44] we have proven that if the intensity of the spatial saddle points on a critical curve is parametrised by scale, scale space saddles are in fact the extrema of the parametrisation.

2.3 Catastrophe Theory

The spatial critical points of a function with non-zero eigenvalues of the Hessian are called *Morse critical points*. The *Morse Lemma* states that at these points the qualitative properties of the function are determined by the quadratic part of the Taylor expansion of this function. This part can be reduced to the *Morse canonical form* by a slick choice of coordinates.

If at a spatial critical point the Hessian degenerates, so that at least one of the eigenvalues is zero, the type of the spatial critical point cannot be determined.

Definition 8 *The* catastrophe points *of* $L(\mathbf{x};t_0)$ *are defined as the points where both the spatial gradient and the determinant of the Hessian vanish:* $\nabla L(\mathbf{x};t_0)=0$ *and* $\det H(\mathbf{x};t_0)=0$.

The term catastrophe was introduced by Thom [63,64]. It denotes a (sudden) qualitative change in an object as the parameters on which this object depends change smoothly. This behaviour was already known by the terms perestroika, bifurcation and metamorphosis. The name catastrophe theory was suggested by Zeeman [70] to unify singularity theory, bifurcation theory and their applications and gained wide popularity. A thorough mathematical treatment on singularity theory can be found in the work of Arnol'd [2–7]. More pragmatic introductions and applications are widely published, e.g. [9,24,26,52,59,70].

The catastrophe points are also called *non-Morse critical points*, since a higher order Taylor expansion is essentially needed to describe the qualitative properties. Although the dimension of the variables is arbitrary, the *Thom Splitting Lemma* states that one can split up the function in a Morse and a non-Morse part. The latter consists of variables representing the k "bad" eigenvalues of the Hessian that become zero. The Morse part contains the $n-k$ remaining variables. Consequently, the Hessian contains a $(n-k)\times(n-k)$ sub-matrix representing a Morse function. It therefore suffices to study the part of k variables. The canonical form of the function at the non-Morse critical point thus contains two parts: a Morse canonical form of $n-k$ variables, in terms of the quadratic part of the Taylor series, and a non-Morse part. The latter can by put into canonical form called the *catastrophe germ*, which is obviously a polynomial of degree 3 or higher.

Since the Morse part does not change qualitatively under small perturbations, it is not necessary to further investigate this part. The non-Morse part, however, does change. Generally the non-Morse critical point will split into a non-Morse critical point, described by a polynomial of lower degree, and Morse critical points, or even exclusively into Morse critical points. This event is called a *morsification*. So the non-Morse part contains the catastrophe germ and a perturbation that controls the morsifications.

Then the general form of a Taylor expansion $f(\mathbf{x})$ at a non-Morse critical point of an n dimensional function can be written as (*Thom's Theorem*):

$$f(\mathbf{x};\lambda)=CG(x_1,\ldots,x_k)+PT(x_1,\ldots,x_k;\lambda_1,\ldots,\lambda_l)+\sum_{i=k+1}^{n}\epsilon_i x_i^2, \qquad (2)$$

where $CG(x_1,\ldots,x_k)$ denotes the catastrophe germ, $PT(x_1,\ldots,x_k;\lambda_1,\ldots,\lambda_l)$ the perturbation germ with an l-dimensional space of parameters, and in the Morse part $\epsilon_i=\pm 1$. In Table 1 the germs with $l\leq 4$ are listed. In 2D these form, together with $A_1^{\pm}\stackrel{\text{def}}{=}\pm x^2\pm y^2$ and taking D_4^+ and D_4^- together as $D_4^{\pm}$,

name	nickname	CG	PT
A_2	Fold	x^3	$\lambda_1 x$
$A_3^{\pm}$	Cusp	$\pm x^4$	$\lambda_1 x + \lambda_2 x^2$
A_4	Swallowtail	x^5	$\lambda_1 x + \lambda_2 x^2 + \lambda_3 x^3$
$A_5^{\pm}$	Butterfly	$\pm x^6$	$\lambda_1 x + \lambda_2 x^2 + \lambda_3 x^3 + \lambda_4 x^4$
D_4^{+}	Hyperbolic Umbilic	$x^2 y + y^3$	$\lambda_1 x + \lambda_2 y + \lambda_3 x^2$
D_4^{-}	Elliptic Umbilic	$x^2 y - y^3$	$\lambda_1 x + \lambda_2 y + \lambda_3 x^2$
$D_5^{\pm}$	Parabolic Umbilic	$x^2 y \pm y^4$	$\lambda_1 x + \lambda_2 y + \lambda_3 y^2 + \lambda_4 x^2$

Table 1
Description of non-Morse critical points for maximal 4 different perturbation parameters. Each contain a catastrophe germ (CG) and corresponding perturbation term (PT).

the so-called *Thom's seven*.

These germs are the starting point of the infinite set of so-called simple real singularities, whose catastrophe germs are given by the infinite series $A_k^{\pm} \stackrel{\text{def}}{=} \pm x^{k+1}, k \geq 1$ and $D_k^{\pm} \stackrel{\text{def}}{=} x^2 y \pm y^{k-1}, k \geq 4$, and the three exceptional singularities $E_6 \stackrel{\text{def}}{=} x^3 \pm y^4$, $E_7 \stackrel{\text{def}}{=} x^3 + xy^3$, and $E_8 \stackrel{\text{def}}{=} x^3 + y^5$. The germs A_k^{+} and A_k^{-} are equivalent for $k = 1$ and k even.

2.3.1 Catastrophes and Scale Space

In Definition 8, the number of equations defining the catastrophe point equals $n+1$ and therefore it is over-determined with respect to the n spatial variables. Consequently, catastrophe points are generically not found in typical images. In scale space, however, the number of variables equals $n+1$ and catastrophes occur as isolated points.

Although the list of catastrophes starts very simple, it is not trivial to apply it directly to scale space by assuming that scale is just one of the perturbation parameters.

For example, in one-dimensional images the Fold catastrophe reduces to $x^3 + \lambda x$. It describes the change from a situation with two critical points (a maximum and a minimum) for $\lambda < 0$ to a situation without critical points for $\lambda > 0$. See *e.g.* Figure 1 in Section 3.1.1 for an example of such an annihilation sequence. This event can occur in two ways. The extrema are annihilated for increasing λ, but the opposite – creation of two extrema for decreasing λ – is also possible.

In scale space, however, there is an extra constraint: the germ has to satisfy the

diffusion equation. Thus the catastrophe germ x^3 implies an extra term $6xt$. On the other hand, the perturbation term is given by $\lambda_1 x$, so by taking $\lambda = 6t$ scale plays the role of the perturbing parameter. This gives a directionality to the perturbation parameter, in the sense that the only remaining possibility for this A_2-catastrophe in one-dimensional images is an annihilation.

In higher dimensional images also the opposite – *i.e.* a Fold catastrophe describing the creation of a pair of critical points – is possible. Then the perturbation $\lambda = -6t$ with increasing t requires an additional term of the form $-6xy^2$ in order to satisfy the diffusion equation, see Definition 9.

The transfer of the catastrophe germs to scale space has been made by many authors, [10–12,16,34–38,43–46,48,50], among whom Damon's account is probably the most rigorous. He showed that the only generic morsifications in scale space are the aforementioned Fold catastrophes describing *annihilations* and *creations* of pairs of critical points. These two points have opposite sign of the determinant of the Hessian before annihilation and after creation. All other events are compounds of such events. It is however possible that one may not be able to distinguish these generic events, *e.g.* due to numerical limitations, coarse sampling, or (almost) symmetries in the image.

Definition 9 *The scale space catastrophe germs are defined by*

$$f^{A}(\mathbf{x};t) \stackrel{\text{def}}{=} x_1^3 + 6x_1 t + Q(\mathbf{x};t)\,,$$
$$f^{C}(\mathbf{x};t) \stackrel{\text{def}}{=} x_1^3 - 6x_1 t - 6x_1 x_2^2 + Q(\mathbf{x};t)\,.$$

The quadratic term $Q(\mathbf{x};t)$ is defined

$$Q(\mathbf{x};t) \stackrel{\text{def}}{=} \sum_{i=2}^{n} \epsilon_i (x_i^2 + 2t),$$

where $\sum_{i=2}^{n} \epsilon_i \neq 0$ and $\epsilon_i \neq 0\ \forall i$.

Note that the scale space catastrophe germs f^{A} and f^{C}, and the quadratic term Q satisfy the diffusion equation. The germs f^{A} and f^{C} correspond to the two qualitatively different Fold catastrophes at the origin, an annihilation and a creation respectively. From Definition 9 it is obvious that annihilations occur in any dimension, but creations require at least 2 dimensions. Consequently, in 1D signals only annihilations occur. Furthermore, for images of arbitrary dimension it suffices to investigate the 2D case due to the Splitting Lemma.

2.3.2 The Annihilation Germ

Spatial critical points at any scale t for f^{A} follow directly from $\nabla f^{\mathrm{A}}(\mathbf{x};t)=0$:

$$\begin{cases} 3x_1^2 = -6t \\ 2\epsilon_i x_i = 0, \quad i \geq 2 \end{cases}$$

Then the critical curve is parametrised by $(\pm\sqrt{-2t},0,\ldots,0;t), t \leq 0$. At the origin a catastrophe takes place. The determinant of the Hessian is given by $\det H = cx_1$, with the constant $c = 3\cdot 2^n \Pi_{i=2}^n \epsilon_i$. So two critical points with opposite sign approach the origin as t increases to zero. Note that $\operatorname{tr} H = 6x_1 + \sum_{i=2}^n 2\epsilon_i$, which is generically non-zero at catastrophe points. This explains the constraints on the ϵ_i in Definition 9.

2.3.3 The Creation Germ

The creation germ is a bit more complicated. Spatial critical points at any scale t for f^{C} follow from $\nabla f^{\mathrm{C}}(\mathbf{x};t)=0$:

$$\begin{cases} 3x_1^2 - 6x_2^2 = 6t \\ 2x_2(\epsilon_2 - 6x_1) = 0 \\ 2\epsilon_i x_i = 0,\ i \geq 3 \end{cases}$$

Since we look in the neighbourhood of the origin, we take $x_2 = 0$. Then the critical curve is parametrised by $(\pm\sqrt{2t},0,\ldots,0;t), t \geq 0$. At the origin a catastrophe takes place. The determinant of the Hessian is given by $\det H = cx_1(\epsilon_2 - 6x_1) - 12cx_2^2$, with the constant $c = 3\cdot 2^n \Pi_{i=3}^n \epsilon_i$, so two critical points with opposite sign leave the origin as t increases from zero. Note that this catastrophe is a Fold catastrophe since it describes the creation of two critical points, although there is a striking resemblance to the description of the Elliptic Umbilic catastrophe. Furthermore, the description of the catastrophe is essentially local: If t is taken too large, the (non-generic) degeneration of the Hessian at $x_1 = \frac{1}{6}\epsilon_2$ has to be taken into account. We will elaborate on these items in Section 3.

2.4 Scale Space Hierarchy

From the previous section it follows that each critical curve in $(\mathbf{x};t)$-space consists of separate branches, each of which is defined from a creation event

to an annihilation event. We set $\#_C$ the number of creation events on a critical path and $\#_A$ the number of annihilation events. Since there exists a scale at which only one spatial critical point (an extremum) remains (see Loog *et al.* [51]), there is exactly one critical path with $\#_A = \#_C$, whereas all other critical paths have $\#_A = \#_C + 1$. That is, all but one critical paths are defined for a finite scale range.

One of the properties of scale space is non-enhancement of local extrema. Therefore, iso-intensity manifolds (isophotes in 2D) in the neighbourhood of a spatial extremum at a certain scale t_0 move towards the spatial extremum at coarser scale until at some scale t_1 the intensity of the extremum equals the intensity of the manifold. The iso-intensity surface in scale space forms a dome, with its top at the extremum at scale t_1. Since the intensity of the extremum is monotonically in- or decreasing (depending on whether it is a minimum or a maximum, respectively), all such domes are nested. Retrospectively, each extremum branch carries a series of nested domes, defining increasing regions around the extremum in the input image.

In [44] we have proven that these regions are uniquely related to one extremum as long as the intensity of the domes does not reach that of the so-called critical dome. The latter is formed by the iso-intensity manifold with its top at the extremum and containing a scale space saddle (see section 2.2) that is part of the same critical curve. An example of a critical dome and its related critical curve is shown in Figure 6 in Section 3.2.1.

In this way a hierarchy of regions of the input image is obtained, which can be regarded as a kind of pre-segmentation. It also results in a partition of the scale space itself. Details can be found in [44–46].

The crucial role is played by the scale space saddles and the catastrophe points. As long as only annihilation and creation events occur, the hierarchy is obtained straightforwardly. However, sometimes higher order catastrophes are needed to describe the local structure, *viz.* when two or more catastrophes happen to be almost incident and cannot be segregated due to coarse sampling, numerical imprecision, or (almost) symmetries in the image. In the next section we describe these higher order events.

3 Scale space catastrophes and scale space saddles

In this section we discuss the appearance of catastrophe events in scale space and the effect on scale space saddles. Firstly, results on one-dimensional images are given, because in this particular case scale space saddles coincide with catastrophe points. Secondly, multi-dimensional images are discussed.

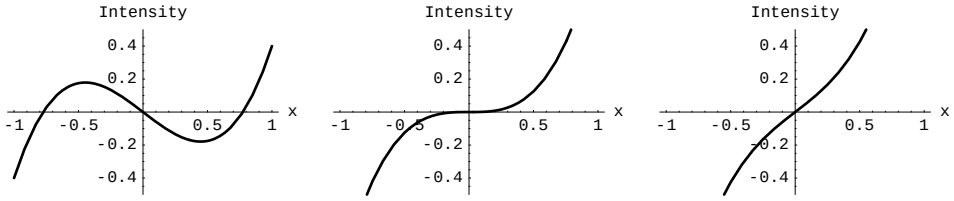

Fig. 1. Fold catastrophe for increasing scales a) t=-1: Two extrema. b) t=0: Catastrophe at the origin. c) t=1: No extrema.

3.1 1D images

In 1D images the critical iso-intensity manifolds (or separatrices) are given by the isophotes through the catastrophes points, since these points are identical to the scale space saddles: $H = L_{xx}$ and $L_t = \Delta L = L_{xx}$. At such points the extended Hessian, Definition 7, reads

$$\mathcal{H} = \begin{pmatrix} 0 & L_{xxx} \\ L_{xxx} & L_{xxxx} \end{pmatrix}.$$

It is generically non-zero at scale space saddles and $\det \mathcal{H} = -L_{xxx}^2 < 0$. In one dimensional images only cuspoid catastrophes (the A_k-type of Table 1) occur, of which we will discuss the Fold A_2 and the Cusp A_3.

3.1.1 Fold catastrophe

The generic annihilation is called a Fold and is defined by (see Definition 9 and further)

$$L(x;t) = x^3 + 6xt\,.$$

The only perturbation parameter is given by t after the identification $\lambda_1 = 6t$. The intensity for increasing scales is shown in Figure 1. It has a scale space saddle if both derivatives are zero, that is,

$$\begin{cases} L_x = 3x^2 + 6t = 0 \\ L_t = 6x \qquad\quad = 0 \end{cases}$$

So it is located at the origin with intensity equal to zero. The determinant of the extended Hessian equals -36, indicating a saddle. A possible parametrisation of the critical curve is $(x(s);t(s)) = (\pm\sqrt{-2s}; s), s \leq 0$ and the cor-

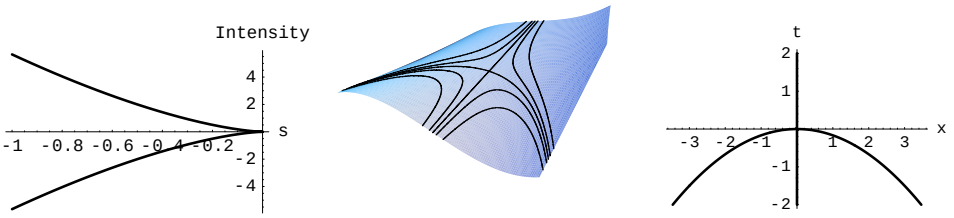

Fig. 2. a) Parametrised intensity of the Fold catastrophe. b) 1+1D intensity scale space surface of the Fold catastrophe in $(x, t, L(x;t))$ space. c) Segments of b), defined by the scale space saddle intensity.

responding parametrised intensity reads $P(s) = \pm 4s\sqrt{-2s}, s \leq 0$, see Figure 2a.

The critical dome is given by the isophotes $L(x;t) = 0$ through the origin, so $(x;t) = (0;t)$ and $(x;t) = (x; -\frac{1}{6}x^2)$. Figure 2b shows isophotes $L = constant$ in the $(x;t, L(x;t))$-space, where the self-intersection of $L = 0$ gives the annihilation point. This isophote gives the separatrices of the different parts of the image. The separation curves in the $(x;t)$-plane are shown in Figure 2c. For $t < 0$, four regions exist, for $t > 0$ two remain (compare to Figure 1a-c).

At the catastrophe point the isophotes of the scale space saddle form a pitchfork. Due to the causality principle it has 3 branches downwards and only one upward, *i.e.* at the scale space saddle four separate regions change to two separate regions. Locally the isophotes are described by $L(x;t) = L_{xt}(\frac{1}{6}x^3 + xt) \stackrel{\text{def}}{=} 0$, so the horizontally traversing branches of the scale space saddle isophote necessarily have branches given by $t = -\frac{1}{6}x^2$, describing the disappearance of two regions.

3.1.2 Cusp catastrophe

Although all catastrophes are generically described by fold catastrophes, one may encounter higher order catastrophes, e.g. due to numerical imprecision or symmetries in the signal, for instance when a set of two minima and one maximum change into one minimum, but one is not able to detect which minimum is annihilated.

The first higher order catastrophe describing such a situation is the Cusp catastrophe. The scale space representation of the catastrophe germ reads $\pm(x^4 + 12x^2t + 12t^2)$, the perturbation term was given by $\lambda_1 x + \lambda_2 x^2$, see Table 1. Obviously, scale fulfils the role of the perturbation by λ_2. Therefore the scale space form is given by

$$L(x;t) = \frac{1}{12}x^4 + x^2t + t^2 + \epsilon x,$$

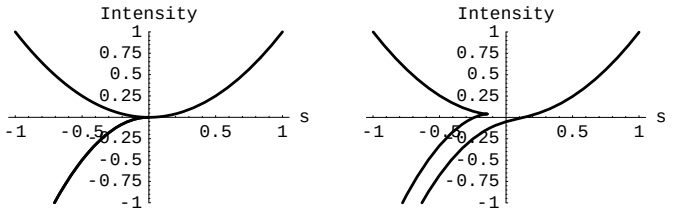

Fig. 3. Parametrised intensity of the Cusp catastrophe a) $\epsilon = 0$ b) $0 <\mid \epsilon \mid \ll 1$

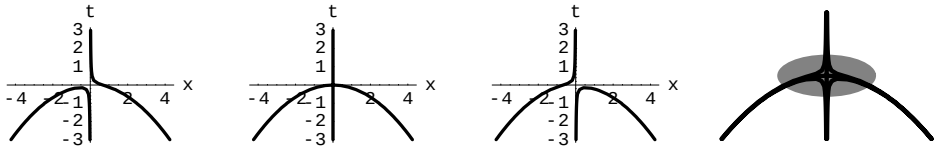

Fig. 4. Critical paths in the $(x;t)$-plane. a) $\epsilon < 0$ b) $\epsilon = 0$ c) $\epsilon > 0$ d) detection of the critical paths around the origin with uncertainty represented by the oval.

where the two perturbation parameters are given by t for the second order term and ϵ for the first order term. Scale space critical points are given by

$$\begin{cases} L_x = \frac{1}{3}x^3 + 2xt + \epsilon = 0 \\ L_t = x^2 + 2t \qquad\quad = 0 \end{cases}$$

If $\epsilon = 0$ the situation as sketched above occurs. The catastrophe takes place at the origin, where two minima and a maximum change into one minimum for increasing t. At the origin also $L_{xxx} = 0$, resulting in a zero eigenvalue of the extended Hessian. Note that this degeneration is automatically induced by the Cusp catastrophe. The parametrised intensity curves $(L_1(0;s) = s^2, \forall s$ and $L_2(\pm\sqrt{-6s};s) = -2s^2, s \leq 0)$ are shown in Figure 3a. Note that at the bottom left the two branches of the two minima with equal intensity, given by L_2, coincide. The case $0 <\mid \epsilon \mid \ll 1$, where a morsification has taken place, is visualised in Figure 3b. This Figure shows the remaining Fold catastrophe of a minimum and a maximum (compare to Figure 2a), and the unaffected other minimum.

It is this splitting that may not be discernible in practice, although it is the generic situation. Depending on the value and sign of ϵ one can find the three different types of catastrophe shown in Figure 4a-c. With an uncertainty in the measurement they may coincide, as shown in Figure 4d, where the oval represents the possible measure uncertainty.

With the degeneration of the extended Hessian at the origin if $\epsilon = 0$, also the shape of the isophotes changes as shown in Figure 5. Since one eigenvalue is zero, the only remaining eigenvector is parallel to the x-axis. So there is no critical isophote in the t-direction, but both parts pass the origin horizontally. Consequently, three regions disappear. Furthermore the annihilating minimum

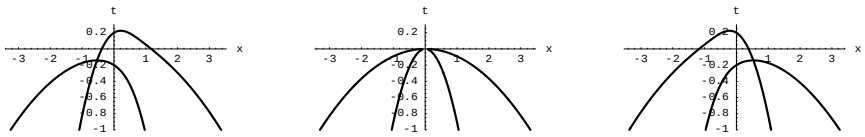

Fig. 5. Critical isophotes in the $(x;t)$-plane. a) $\epsilon < 0$ b) $\epsilon = 0$ c) $\epsilon > 0$

cannot be distinguished from the remaining minimum.

3.1.3 Higher order Cuspoids

One can easily verify that higher order Cuspoids, A_k, $k > 3$, correspond to the annihilation of k regions simultaneously. Morsification per perturbation parameter leads to A_l, $l < k$ catastrophes, and a complete morsification yields only Fold catastrophes.

3.2 n-D images, n > 1

In higher dimensions the structure is more complicated, since generically scale space saddles do not coincide with catastrophe points. For n-D images, $n > 1$, it suffices to investigate scale space critical points in 2+1D, since the first seven elementary catastrophes can locally be written in 2 dimensions. Apart from the in one dimension determined cuspoid catastrophes A_k causing annihilations, also umbilic catastrophes D_k occur, requiring 2 variables (see Table 1). The first two types are the hyperbolic D_4^+ and the elliptic D_4^- umbilic catastrophes.

If we assume $L_{yy} = -L_{xx}$ so that $\Delta L = 0$, the extended Hessian, Definition 7, becomes

$$\mathcal{H} = \begin{pmatrix} L_{xx} & L_{xy} & L_{xt} \\ L_{xy} & -L_{xx} & L_{yt} \\ L_{xt} & L_{yt} & L_{tt} \end{pmatrix}.$$

The determinant is $-L_{tt}\left(L_{xx}^2 + L_{xy}^2\right) + L_{xx}\left(L_{xt}^2 - L_{yt}^2\right) + 2\, L_{xt}L_{xy}L_{yt}$ and the trace simplifies to L_{tt}. Both are generically non-zero.

In this section we subsequently describe the scale space representations in 2+1D of the cuspoid catastrophes A_2 and A_3, and the umbilic catastrophes D_3^+ and D_3^-, together with their morsifications, the appearances of scale space saddles and the possibilities with respect to the degeneration of $\mathcal{H}$.

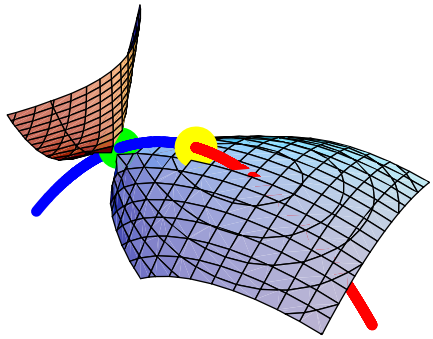

Fig. 6. The critical curve contains a catastrophe point (bright dot) and a scale space saddle (dark dot). The iso-intensity surface through the scale space saddle contains two parts touching each other at the scale space saddle. One part is dome-shaped and intersects the critical curve at the top of the dome.

3.2.1 Fold catastrophe

The first type of catastrophes is given by the Fold catastrophe, which follows directly from Table 1 and Eq. (2) and was given in n-D in Section 2.3.2:

$$L(x, y; t) = x^3 + 6xt + \alpha(y^2 + 2t), \tag{3}$$

where $\alpha = \pm 1$. Positive sign describes a saddle – minimum annihilation, negative sign a saddle – maximum annihilation. Without loss of generality we take $\alpha = 1$. Then

$$\begin{cases} L_x = 3x^2 + 6t \\ L_y = 2y \\ L_t = 6x + 2 \\ \det(H) = 12x \\ \det(\mathcal{H}) = -72, \end{cases}$$

so the catastrophe takes place at the origin with intensity equal to zero and the scale space saddle is located at $(x, y; t) = (-\frac{1}{3}, 0; -\frac{1}{18})$ with intensity $-\frac{1}{27}$. The surface $L(x, y; t) = -\frac{1}{27}$ through the scale space saddle is shown in Figure 6. It has a local maximum at $(x, y; t) = (\frac{1}{6}, 0; -\frac{1}{72})$: the top of the extremum dome. Recall that the coordinates have no quantitative significance.

The iso-intensity surface through the scale space saddle can be visualised by two surfaces touching each other at the scale space saddle. One part of the

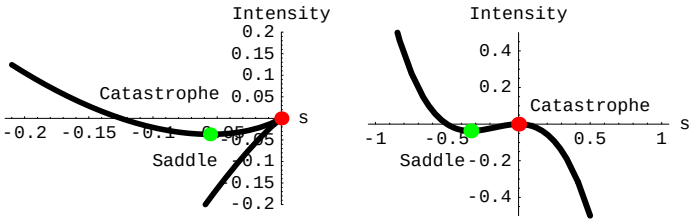

Fig. 7. Intensity of the critical curve, parametrised by a) the x-coordinate and b) the t-coordinate. Both showing at the origin an annihilation, at the minimum the scale space saddle.

surface is related to the extremum corresponding to the scale space saddle. The other part encircles some other segment of the image. The surface belonging to the extremum forms a dome. The critical curve intersects this surface twice. The saddle branch has an intersection at the scale space saddle, the extremum branch at the top of the dome, as shown in Figure 6.

A parametrisation of the two branches of the critical curve is given by $(x(s), y(s); t(s)) = (\pm\sqrt{-2s}, 0; s), s \leq 0$.

The intensity of the critical curve reads $L(s) = 2s \pm 4s\sqrt{-2s}, s \leq 0$ (with $\partial_s t = 1$ and $\partial_s L = \Delta L \cdot \partial_s t = 2 \pm 6\sqrt{-2s}$). The scale space saddle is located at $s = -\frac{1}{18}$, the catastrophe at the local maximum, the connection of the two intensity-curves, $s = 0$. These points are visible in Figure 7a as the local minimum of the parametrisation curve and the connection point of the two curves, the upper branch representing the spatial saddle, the lower one the minimum.

Note that an alternative parametrisation of both branches of the critical curve simultaneously is given by $(x(s), y(s); t(s)) = (s, 0; -\frac{1}{2}s^2)$. Then the intensity of the critical curve is given by $L(s) = -2s^3 - s^2$. Now $\partial_s t = -s$ and $\partial_s L(s) = -6s^2 - 2s = (6s + 2)(-s)$ and the latter is still equivalent to $\Delta L \cdot t_s$. The catastrophe takes place at $s = 0$, the saddle at $s = -\frac{1}{3}$. These points are visible in Figure 7b as the extrema of the parametrisation curve. The branch $s < 0$ represents the saddle point, the branch $s > 0$ the minimum.

3.2.2 Cusp catastrophe

With the similar argumentation as in the one-dimensional case it is also interesting to investigate the behaviour around the next catastrophe event. The higher-dimensional cusp catastrophe in scale space follows directly from Table 1 and Eq. (2). It is the 2-D scale space extension of the catastrophe discussed in section 3.1.2 and is defined by

$$L(x, y; t) = \frac{1}{12}x^4 + x^2 t + t^2 + \alpha(2t + y^2) + \epsilon x$$

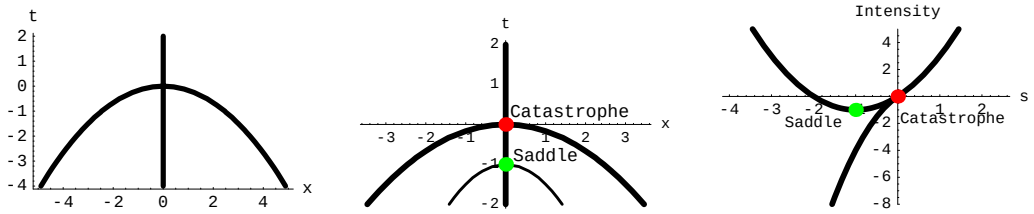

Fig. 8. a) Critical paths. b) Critical paths with zero-Laplacean, catastrophe point and scale space saddle if $\alpha > 0$. c) Intensity of the critical paths. The part bottom-left represents two branches ending at the catastrophe point.

where, again, $\alpha = \pm 1$. If $\epsilon \neq 0$ a fold catastrophe results. Then

$$\begin{cases} L_x = \frac{1}{3}x^3 + 2xt + \epsilon \\ L_y = 2\alpha y \\ L_t = x^2 + 2\alpha + 2t \\ \det(H) = 2\alpha(x^2 + 2t) \\ \det(\mathcal{H}) = 4\alpha(2t - x^2). \end{cases}$$

The critical curves in the $(x;t)$-plane at $\epsilon = 0, y = 0$ are shown in Figure 8a. They form a so-called pitchfork bifurcation at the origin, the catastrophe point.

Critical points are on the curves given by $(x(s), y(s); t(s)) = (0, 0; s)$ and $(x(s), y(s); t(s)) = (\pm\sqrt{-6s}, 0; s), s \leq 0$.

The intensities are given by $L_1(s) = L(0, 0; s) = s^2 + 2\alpha s$ with its extremum at $s = -\alpha$ and $L_2(s) = L(\pm\sqrt{-6s}, 0; s) = -2s^2 + 2\alpha s, s \leq 0$. The latter has an extremum at $s = \frac{1}{2}\alpha$. Since $s \leq 0$, these scale space saddles only occur if $\alpha < 0$. It is therefore essential to distinguish between the two signs of α.

3.2.2.1 Case $\alpha > 0$ For positive α, the curve $(x, y; t) = (0, 0; s)$ contains saddles if $t < 0$ and minima if $t > 0$. The other curve contains minima on both branches. At the origin a catastrophe occurs, at $(x, y; t) = (0, 0, -\alpha)$ a scale space saddle, see Figure 8b. The intensities of the critical curves are shown in Figure 8c; The two branches of the minima for $t < 0$ have equal intensity. The iso-intensity manifold in scale space forms a double dome since the two minima are indistinguishable, see Figure 9.

A small perturbation ($0 <| \epsilon | \ll 1$) leads to a generic image containing a Fold catastrophe and thus a single cone. However, as argued in section 3.1.2 this perturbation may be too small to identify the annihilating minimum. We will

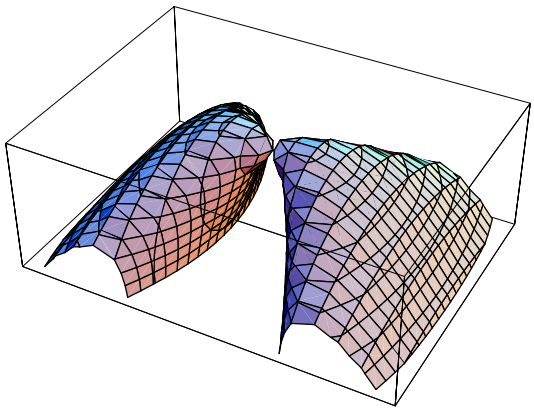

Fig. 9. 2D Surface trough the scale space saddle at a Cusp catastrophe, $\alpha > 0$.

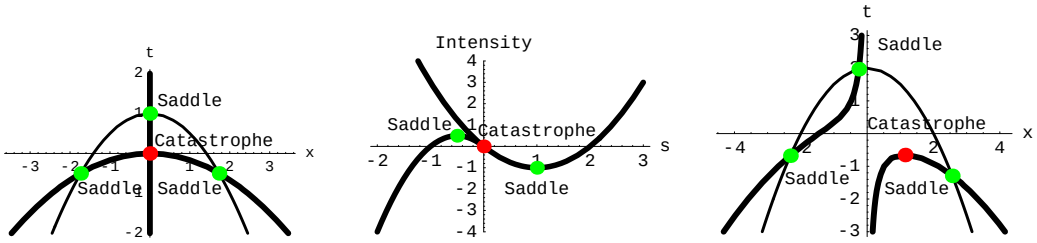

Fig. 10. a) Critical paths with zero-Laplacean, catastrophe point and scale space saddle if $\alpha = -1$. b) Intensity of the critical paths. The part bottom-left represents two branches ending at the catastrophe point. c) Critical paths with $\alpha < 0$, $9\epsilon^2 < -16\alpha^3$, zero-Laplacean, catastrophe point and scale space saddle.

use this degeneration in Section 4 to identify multiple regions with one scale space saddle.

3.2.2.2 Case $\alpha < 0$ If α is negative, the curve $(x, y; t) = (0, 0; s)$ contains a maximum if $t < 0$ and a saddle if $t > 0$, while the curve $(x, y; t) = (\pm\sqrt{-6s}, 0; s), s < 0$ contains saddles. Now 3 scale space saddles occur: at $(x, y; t) = (0, 0; -\alpha)$ and $(x, y; t) = (\pm\sqrt{-3\alpha}, 0; \frac{1}{2}\alpha)$, see Figure 10a. The corresponding intensities are shown in Figure 10b, where again the intensities of the two saddle branches (and thus the scale space saddles) for $t < 0$ coincide.

The iso-intensity surfaces through the scale space saddles are shown in Figure 11. The scale space saddles at $t = \frac{1}{2}\alpha$ both encapsulate the maximum at the t-axis. The scale space saddle at $t = -\alpha$ is *void*, *i.e.* it is not related to an extremum. This is clear from the fact that there is only one extremum present.

If a small perturbation $(0 <| \epsilon |\ll 1)$ is added the three scale space saddles remain present in the generic image. Their trajectories in the $(x; t)$-plane are shown in Figure 10c. Now a Fold catastrophe is apparent, but also a saddle branch containing two (void) scale space saddles, caused by the neighbourhood of the annihilating saddle-extremum pair.

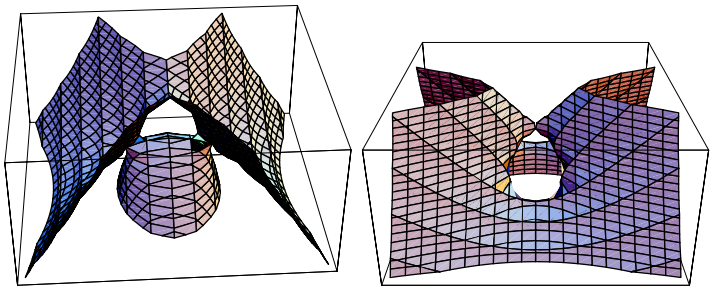

Fig. 11. 2D Iso-intensity manifold trough the scale space saddles a) at $t = -\frac{1}{2}$ and b) at $t = 1$

3.2.2.3 Degeneration of $\det(\mathcal{H})$ The extended Hessian degenerates if its determinant vanishes, *i.e.* if $4\alpha(2t - x^2) = 0$. This implies $2t = x^2$. Then $L_x = 0$ reduces to $\frac{4}{3}x^3 + \epsilon = 0$. For $\epsilon = 0$ the degeneration takes place at the origin, that is, at the cusp catastrophe. But then $x = 0, t = 0$ and $L_t = 0$ implies $\alpha = 0$, which is non-generic. For other arbitrary values of ϵ, $L_t = 0$ implies $x^2 = -\alpha$, so it is located at $(x, y; t) = (-\mathrm{sgn}\,(\epsilon)\sqrt{-\alpha}, 0, -\frac{1}{2}\alpha)$, where $\alpha < 0$ and $9\epsilon^2 = -16\alpha^3$.

This special value is located at the non-annihilating saddle branch where the two scale space saddle points coincide, *i.e.* where the saddle branch touches the zero-Laplacean. This case is non-generic, since the intersection of the critical curve and the hyper-plane $\Delta L = 0$ at this value is not transverse. This value describes the transition of the case with two void scale space saddles to the case without scale space saddles: For $\mid \epsilon \mid < \frac{4}{3}\sqrt{-\alpha^3}$ two void scale space saddles occur on the non-annihilating saddle branch as shown in Figure 10c. For $\mid \epsilon \mid > \frac{4}{3}\sqrt{-\alpha^3}$ none occur since the saddle branch does not intersect the zero-Laplacean. In other words: a Fold catastrophe *in scale space* occurs, regarding two scale space critical points (*i.e.* saddles) with different signs of $\det(\mathcal{H})$ and controlled by the perturbation parameter ϵ.

3.2.3 Hyperbolic umbilic catastrophe

The hyperbolic umbilic catastrophe germ is given by $x^3 + xy^2$. Its scale space addition is $8xt$. The perturbation term contains three terms: $\lambda_1 x + \lambda_2 y + \lambda_3 y^2$. Obviously scale takes the role of λ_1. The scale space hyperbolic umbilic catastrophe germ with perturbation is thus defined by

$$L(x, y; t) = x^3 + xy^2 + 8xt + \alpha(y^2 + 2t) + \beta y$$

where the first three terms describe the scale space catastrophe germ. The set (α, β) form the extra perturbation parameters. Then

$$\begin{cases} L_x = 3x^2 + 8t + y^2 \\ L_y = 2xy + 2\alpha y + \beta \\ L_t = 8x + 2\alpha \\ \det(H) = 12x(x+\alpha) - 4y^2 \\ \det(\mathcal{H}) = -128(x+\alpha). \end{cases}$$

One can verify that at the combination $(\alpha, \beta) = (0, 0)$ four critical points exist for each $t < 0$. At $t = 0$ the four critical curves given by $(x, y; t) = (\pm\sqrt{-\frac{8}{3}t}, 0; t)$ and $(x, y; t) = (0, \pm\sqrt{-8t}; t)$ annihilate simultaneously at the origin (see *e.g.* Kalitzin [37]). This is non-generic, since this point is a scale space saddle and also $\det(\mathcal{H}) = 0$.

Morsification takes place in two steps. In the first step one perturbation parameter is non-zero. If $\alpha \neq 0$ and $\beta = 0$, the annihilations are separated. At the origin a Fold catastrophe occurs with critical curves $(x, y; t) = (-\sqrt{-\frac{8}{3}t}, 0; t)$. On one of these curves both a scale space saddle at $(x, y; t) = (-\frac{\alpha}{4}, 0; -\frac{3\alpha^2}{128})$, and the other catastrophe at $(x, y; t) = (-\alpha, 0; -\frac{3}{8}\alpha^2)$ are located. At the latter the critical curves $(-\alpha, \pm\sqrt{-3\alpha^2 - 8t}; t), t < -\frac{3}{8}\alpha^2$ annihilate in a (non-generic!) Cusp catastrophe.

If $\alpha = 0$ and $\beta \neq 0$, the double annihilation breaks up into two Fold annihilations with symmetric non-intersecting critical curves. A scale space saddle is not present.

Finally, if both α and β are non-zero, this complete morsification results in the generic case with two critical curves, each of them containing a Fold annihilation. One the two critical curves contains a scale space saddle, located at $(x, y; t) = (-\frac{1}{4}\alpha, -\frac{2\beta}{3\alpha}; -\frac{3\alpha^2}{128} - \frac{\beta^2}{18\alpha^2})$

The extended Hessian degenerates for $x = -\alpha$. Then follows from $L_t = 0$ that $x = \alpha = 0$ and from L_y also $\beta = 0$, which is a non-generic situation.

3.2.4 Elliptic umbilic catastrophes

The elliptic umbilic catastrophe germ is given by $x^3 - 6xy^2$. Its scale space addition is $-6xt$. The perturbation term contains three terms: $\lambda_1 x + \lambda_2 y + \lambda_3 y^2$. Obviously scale takes the role of λ_1. The scale space elliptic umbilic

catastrophe germ with perturbation is thus defined by

$$L(x, y; t) = x^3 - 6xy^2 - 6xt + \alpha(y^2 + 2t) + \beta y \tag{4}$$

where the first three terms describe the scale space catastrophe germ. The set (α, β) form the extra perturbation parameters. Now

$$\begin{cases} L_x = 3x^2 - 6t - 6y^2 \\ L_y = -12xy + 2\alpha y + \beta \\ L_t = -6x + 2\alpha \\ \det(H) = 12x(\alpha - 6x) - 144y^2 \\ \det(\mathcal{H}) = -72(\alpha - 6x). \end{cases}$$

The combination $(\alpha, \beta) = (0, 0)$ gives two critical points for all $t \neq 0$ on the critical curves $(x, y; t) = (0, \pm\sqrt{-t}; t), t < 0$ and $(x, y; t) = (\pm\sqrt{2t}, 0; t), t > 0$. At the origin a so-called scatter event occurs: the critical curve changes from y-axis to x-axis with increasing t. Just as in the hyperbolic case, in fact two Fold catastrophes take place; in this case both an annihilation and a creation.

The morsification for $\alpha = 0$, $\beta \neq 0$ leads to the breaking into two critical curves without any catastrophe: $\det H = 0$ implies $x = y = 0$, but then $L_y = \beta \neq 0$.

The morsification for $\alpha \neq 0$, $\beta = 0$ leads to only one catastrophe event at the origin: the Fold creation. The sign of α determines whether the critical curve contains a maximum – saddle pair or a minimum – saddle pair. Without loss of generality we may choose $\alpha = 1$. For the moment we assume $\beta = 0$ to compare this case with the Fold annihilation. Then the generic creation germ is defined as

$$L(x, y; t) = x^3 - 6xt - 6xy^2 + y^2 + 2t \tag{5}$$

The scale space saddle is located at $(x, y; t) = (\frac{1}{3}, 0; \frac{1}{18})$ and its intensity is $L(\frac{1}{3}, 0; \frac{1}{18}) = \frac{1}{27}$. The surface $L(x, y; t) = \frac{1}{27}$ has a local saddle at $(x, y; t) = (-\frac{1}{6}, 0; \frac{1}{72})$, see Figure 12. At creations newly created extremum domes cannot be present, which is obvious from the non-creation of new level-lines. Whereas annihilations of critical points lead to the annihilations of level-lines, creations of critical points are caused by the rearrangement of already existing level-lines.

This fact becomes clearer if we take a closer look at the structure of the critical curves. The critical curve containing the creation is given by $(x, y; t) =$

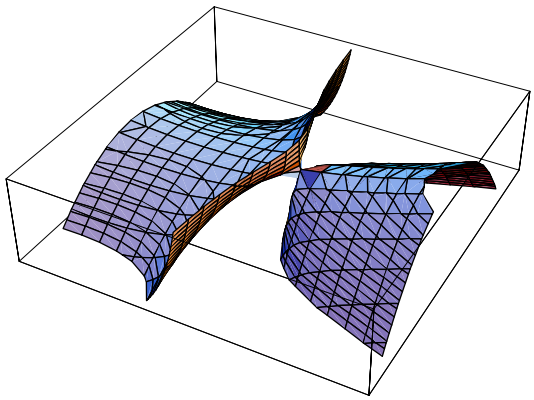

Fig. 12. Iso-intensity surface of the scale space saddle of the creation germ.

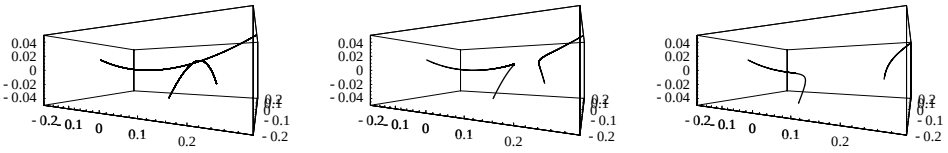

Fig. 13. Critical curves of Eq. (4) with $\alpha = 1$ in $(x, y; t)$-space. a) $\beta = 0$: Degeneration at the connection of the two critical paths b) $0 < \|\beta\| < \frac{1}{32}\sqrt{6}$: Morsification with two catastrophes on one of the critical curves. c) $\|\beta\| > \frac{1}{32}\sqrt{6}$: Morsification without catastrophes on the critical curves.

$(\pm\sqrt{2t}, 0; t)$. The other critical curve given by $(x, y; t) = (\frac{1}{6}, \pm\sqrt{\frac{1}{72} - t}; t)$ represents two branches connected at the second catastrophe, see Figure 13a. This point is located at $(x, y; t) = (\frac{1}{6}, 0; \frac{1}{72})$, is an element of both curves and obviously degenerates the extended Hessian. At this point two saddle points and the created extremum go through a Cusp catastrophe resulting in one saddle. Note that ignoring this catastrophe one would find a sudden change of the extremum into a saddle point while tracing the created critical points. Obviously this catastrophe is located between the creation catastrophe and the scale space saddle. The latter therefore does not invoke a critical dome around the created extremum.

The intensity of the creation pair is given by $L(s) = 2s \pm 4s\sqrt{2s}, s \geq 0$, the intensity of the other pair by $L(s) = \frac{1}{216} + s,\ s \leq \frac{1}{72}$. The intensities of both paths are shown in Figure 14a. A close-up around the catastrophe points is given in Figure 14b.

Note that the intensity curve at the bottom-left of Figure 14a-b contains two saddle branches with equal intensity. Figure 14b shows that at the catastrophe in the origin two curves are created. The saddle curve (the left curve) remains, the extremum one (the lower curve) is annihilated at the second catastrophe with one of the two saddle branches with equal intensity. The other saddle branch continues and contains a scale space saddle.

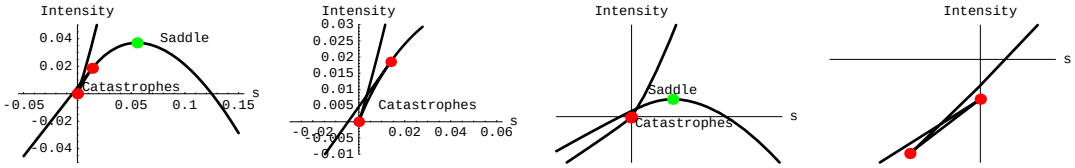

Fig. 14. a) Intensities of critical paths, $\beta = 0$. b) Close-up at both catastrophes, $\beta = 0$. c) Intensities of critical paths, $\beta = \frac{1}{24}\sqrt{2}$. d) Close-up at both catastrophes, $\beta = \frac{1}{24}\sqrt{2}$.

A complete morsification by taking $0 < \|\beta\| \ll 1$ resolves the scatter. It can be shown that the Hessian has two real roots if and only if $\|\beta\| < \frac{1}{32}\sqrt{6}$. At these root points subsequently a creation and an annihilation event take place on a critical curve as shown in Figure 13b. If $\|\beta\| > \frac{1}{32}\sqrt{6}$ the critical curve doesn't contain catastrophe points, see Figure 13c.

If we take $\beta = \frac{1}{24}\sqrt{2}$ the creation is approximately at $(0.013, -0.032; -0.00094)$ and the annihilation is at $(x, y; t) = (1/12, -1/24\sqrt{2}; 0)$. The intensity curves at this situation are visible in Figure 14c-d. Figure 14c shows that the two saddle curve have different intensities and do not coincide. One curve doesn't contain catastrophes, but only one scale space saddle. The other curve contains two catastrophes. A close-up around the catastrophes is shown in Figure 14d.

Due to this morsification the two critical curves do not intersect each other. Also in this perturbed system the minimum annihilates with one of the two saddles, while the other saddle remains unaffected. The scale space saddle remains on the non-catastrophe-involving curve. That is, the creation – annihilation couple and the corresponding saddle branch are not relevant for the scale space saddle and thus the scale space segmentation.

The iso-intensity surface of the scale space saddle due to the creation germ does not contain a dome-shaped surface connected to some other surface, but shows only two parts of the surface touching each other at a void scale space saddle, recall *e.g.* Figure 12.

3.2.5 Higher order Umbilics

One can verify that of the higher order Umbilic catastrophes, $D_k^{\pm}$, $k > 4$, the D_k^+ describe the various annihilations in two dimensions, the compound of (several) Fold catastrophes. The D_k^- introduce complicated scatter-like behaviour which also morsify into Fold catastrophes, but now a combination of both annihilations and creations.

3.3 Morsification summary

All non-Fold catastrophes morsify to Fold catastrophes. The morsification gives insight in the structure around the catastrophe point regarding the critical curves and the scale space saddles. In one dimensional images, catastrophes and scale space saddles coincide. Therefore, at higher catastrophes the extended Hessian necessarily degenerates. These catastrophes, however, give insight in the case where more than two critical points are involved in a complicated annihilation or at several annihilations at almost the same scale space position, without having the ability of distinguish between the Fold pairs.

In higher dimensional images, the cuspoid catastrophes (the A_k) give the same insight, but also allow the assignment of a scale space saddle, and consequently a scale space segment, to more than one extremum. Furthermore the morsification of the Cusp catastrophe showed that it is generic to encounter scale space saddles that are not connected to some dome shaped iso-intensity manifold: the so-called void scale space saddles.

The morsified D_4^- catastrophe describes the creation of two critical points and the annihilation of one of them with another critical point. So while tracing the critical branches of a critical curve both an annihilation and a creation event are traversed.

4 Applications

In this section we give some examples to illustrate the theory presented in the previous sections. To show the effect of a cusp catastrophe in 2D, we firstly take a symmetric artificial image containing two Gaussian blobs and add noise to it. This will make the non-generic symmetric image generic, but in a sense "almost non-generic". This image is shown in Figure 15a. Secondly, the effect is shown on the simulated MR image of Figure 15b. Note that also in this case an almost symmetric, thus non-generic, situation occurs. This image is taken from the web site http://www.bic.mni.mcgill.ca/brainweb.

4.1 Artificial image

Of the noisy image of Figure 15a, a scale space image was built containing 41 scales ranging exponentially from $e^{\frac{10}{8}}$ to $e^{\frac{20}{8}}$. The calculated critical paths are presented in Figure 16a. Ignoring the paths on the border, caused by the extrema in the noise, the paths in the middle of the image clearly show

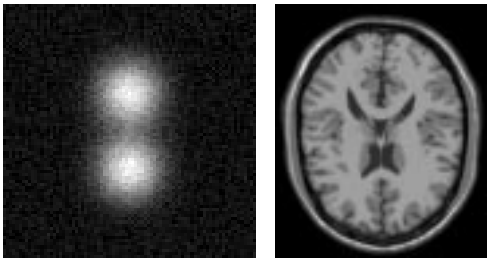

Fig. 15. 2D test images a: Artificial image built by combining two identical blobs and additive noise. b: 181 x 217 artificial MR image.

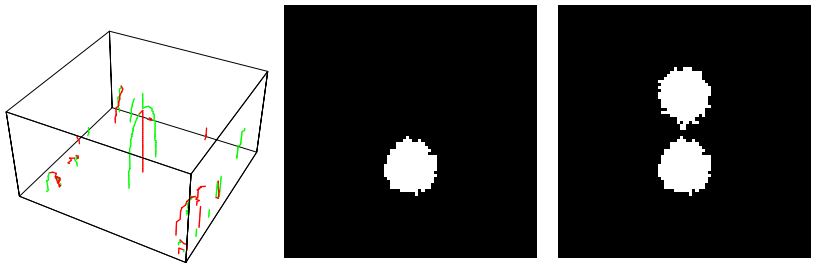

Fig. 16. Example of a Cusp catastrophe: a: Critical paths in scale space. b: Segment according to a Fold catastrophe. c: Segment according to a Cusp catastrophe.

the pitchfork-like behaviour, typical of a non-generic Cusp catastrophe, recall Figure 4. Note that since the symmetric image is perturbed, instead of a cusp catastrophe a fold catastrophe occurs. The scale space saddle on the saddle branch and its intensity define a closed region around the lower maximum, see Figure 16b. For details on how the hierarchy and the segmentation is obtained, *cf.* the algorithm presented in [44]. However, if the noise were slightly different, one could evidently have found the region around the upper maximum instead. Knowing that the image should be symmetric and observing that the critical paths indeed are pitchfork-like, it is thus desirable to label the catastrophe as a Cusp catastrophe. Then the scale space saddle (and its intensity) defines the two regions around both involved extrema, see Figure 16c. This image one would rather expect given Figure 15a.

4.2 Simulated MR image

Subsequently, we took the 2D slice from an artificial MR image shown in Figure 15b. The scale space image at scale 8.37 with the large structures remaining is shown in Figure 17a. Now 7 extrema are found, defining a hierarchy of the regions around these extrema as shown in Figure 17b. In this case is it visually desirable to identify a region to segment S_1 with more or less similar size as region S_3. This is done by assigning a Cusp catastrophe to the annihilation of the extremum of segment S_3, in which the extremum of segment S_1 is also involved. Then the value of the scale space saddle defining segment S_3 also

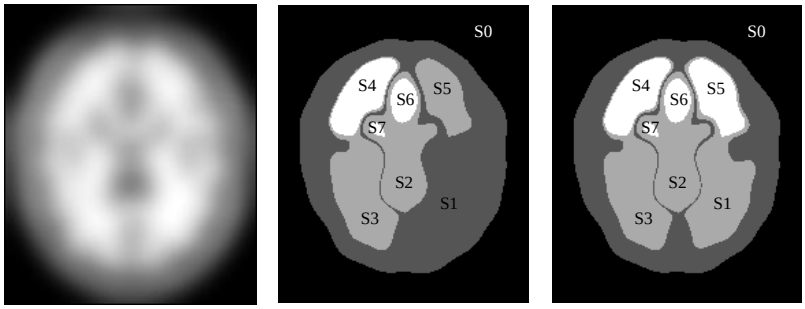

Fig. 17. a) Image on scale 8.4 b) Segments of the 7 extrema of a, assuming that only generic catastrophes occur, which is the actual case in fact. c) Idem, with the iso-intensity manifold of S_1 chosen equally to S_3, *i.e.* after changing the label of a generic event into a non-generic one.

defines an extra region around the extremum in segment S_1. This is shown in Figure 17c, reflecting the symmetry present in Figure 17a. We note that in this example several creation – annihilation events occurred, as described by the morsification of the D_3^- catastrophe.

5 Summary and Discussion

In this paper we investigated the (deep) structure on various catastrophe events in Gaussian scale space. Although it is known that pairs of critical points are annihilated or created (the latter if the dimension of the image is 2 or higher), it is important to describe the local structure of the image around these events. The importance of this local description follows from its significance in building a scale space hierarchy. This algorithm depends on the critical curves, their catastrophe points and the space space saddle points. We therefore embedded the mathematically known catastrophes as presented in section 2 in the framework of linear scale space images.

Firstly, annihilations of extrema can occur in the presence of other extrema. In some cases it is not possible to identify the annihilating extremum due to numerical limitations, coarse sampling, or symmetries in the image. Then the event is described by a Cusp catastrophe instead of a Fold catastrophe. This description is sometimes desirable, *e.g.* if prior knowledge is present and one wishes to maintain the symmetry in the image. The scale space hierarchy can easily be adjusted to this extra information. We gave examples in section 4 on an artificial image and a simulated MR image. We discussed the A_4 and the D_3^+ for this purpose, but the higher order catastrophes in the sequences $A_k, k > 4$ and $D_k^+, k > 3$ can be dealt with in a similar fashion.

Secondly, the morsification of the D_3^- catastrophe was discussed, showing he successive appearance of a creation – annihilation event on a critical curve.

This doesn't influence the hierarchical structure nor the pre-segmentation, but is only important with respect to the movement of the critical curve in scale space. We showed that this appearance heavily depends on the morsification parameters.

The theory described in this paper extends the knowledge of the deep structure of Gaussian scale space. It embeds higher order catastrophes within the framework of a scale space hierarchy. It explains how these events can in principle be used for segmentation, interpreted and implemented, *e.g.* if prior knowledge is available.

References

[1] L. Alvarez and J. Morel. Morphological approach to multiscale analysis: From principles to equations. In *ter Haar Romeny, [29]*, pages 101–112, 1994.

[2] V. I. Arnold, editor. *Geometrical Methods in the Theory of Ordinary Differential Equations*, volume 250 of *Grundlehren der mathematischen Wissenschaften: A Series of Comprehensive Studies in Mathematics*. Springer-Verlag, Berlin, 1983.

[3] V. I. Arnold. *Catastrophe Theory*. Springer, Berlin, 1984.

[4] V. I. Arnold, editor. *Ordinary Differential Equations*. Springer-Verlag, Berlin, 1992.

[5] V. I. Arnold, editor. *Dynamical Systems VI: Singularity Theory I*, volume 6 of *Encyclopaedia of Mathematical Sciences*. Springer-Verlag, Berlin, 1993.

[6] V. I. Arnold, editor. *Dynamical Systems VIII: Singularity Theory II & Applications*, volume 39 of *Encyclopaedia of Mathematical Sciences*. Springer-Verlag, Berlin, 1993.

[7] V. I. Arnold, editor. *Dynamical Systems V: Bifurcation Theory and Catastrophe Theory*, volume 5 of *Encyclopaedia of Mathematical Sciences*. Springer-Verlag, Berlin, 1994.

[8] R. van den Boomgaard and A. Smeulders. The morphological structure of images: The differential equations of morphological scale-space. *IEEE Transactions on Pattern Analysis and Machine Intelligence*, 16(11):1101–1113, 1994.

[9] J.W. Bruce and P.J. Giblin. *Curves and Singularities*. Cambridge University Press, 1984.

[10] J. Damon. Local Morse theory for solutions to the heat equation and Gaussian blurring. *Journal of Differential Equations*, 115(2):386–401, 1995.

[11] J. Damon. Generic properties of solutions to partial differential equations. *Arch. Rat. Mech. Anal.*, pages 353–403, 1997.

[12] J. Damon. Local Morse theory for Gaussian blurred functions. In *Sporring et al. [62]*, pages 147–162, 1997.

[13] J. Duncan and N. Ayache. Medical image analysis: Progress over two decades and the challenges ahead. *IEEE Transactions on Pattern Analysis and Machine Intelligence*, 22(1):85–105, 2000.

[14] L. M. J. Florack. *Image Structure*, volume 10 of *Computational Imaging and Vision Series*. Kluwer Academic Publishers, Dordrecht, The Netherlands, 1997.

[15] L. M. J. Florack. Non-linear scale-spaces isomorphic to the linear case with applications to scalar, vector and multispectral images. *International Journal of Computer Vision*, 42(1/2):39–53, 2001.

[16] L. M. J. Florack and A. Kuijper. The topological structure of scale-space images. *Journal of Mathematical Imaging and Vision*, 12(1):65–80, February 2000.

[17] L. M. J. Florack, R. Maas, and W. J. Niessen. Pseudo-linear scale space theory. *International Journal of Computer Vision*, 31(2/3):247–259, 1999.

[18] L. M. J. Florack, A. H. Salden, B. M. ter Haar Romeny, J. J. Koenderink, and M. A. Viergever. Nonlinear scale-space. *Image and Vision Computing*, 13(4):279–294, May 1995.

[19] L. M. J. Florack, B. M. ter Haar Romeny, J. J. Koenderink, and M. A. Viergever. Scale and the differential structure of images. *Image and Vision Computing*, 10(6):376–388, July/August 1992.

[20] L. M. J. Florack, B. M. ter Haar Romeny, J. J. Koenderink, and M. A. Viergever. Cartesian differential invariants in scale-space. *Journal of Mathematical Imaging and Vision*, 3(4):327–348, 1993.

[21] L. M. J. Florack, B. M. ter Haar Romeny, J. J. Koenderink, and M. A. Viergever. General intensity transformations and differential invariants. *Journal of Mathematical Imaging and Vision*, 4(2):171–187, May 1994.

[22] L. M. J. Florack, B. M. ter Haar Romeny, J. J. Koenderink, and M. A. Viergever. Linear scale-space. *Journal of Mathematical Imaging and Vision*, 4(4):325–351, 1994.

[23] L. M. J. Florack, B. M. ter Haar Romeny, J. J. Koenderink, and M. A. Viergever. The Gaussian scale-space paradigm and the multiscale local jet. *International Journal of Computer Vision*, 18(1):61–75, April 1996.

[24] A. T. Fomenko and T. L. Kunii. *Topological Modeling for Visualization*. Springer-Verlag, Tokyo, 1997.

[25] J. Gauch. Image segmentation and analysis via multiscale gradient watershed hierachies. *IEEE Transactions on Image Processing*, 8(1):69 –79, January 1999.

[26] R. Gilmore. *Catastrophe Theory for Scientists and Engineers*. Dover, 1993. Originally published by John Wiley & Sons, New York, 1981.

[27] L. D. Griffin and A. Colchester. Superficial and deep structure in linear diffusion scale space: Isophotes, critical points and separatrices. *Image and Vision Computing*, 13(7):543–557, September 1995.

[28] L. D. Griffin, A. Colchester, and G. Robinson. Scale and segmentation of grey-level images using maximum gradient paths. *Image and Vision Computing*, 10(5):389–402, 1992.

[29] B. M. ter Haar Romeny, editor. *Geometry-Driven Diffusion in Computer Vision*, volume 1 of *Computational Imaging and Vision Series*. Kluwer Academic Publishers, Dordrecht, 1994.

[30] B. M. ter Haar Romeny, L. M. J. Florack, J. J. Koenderink, and M. A. Viergever, editors. *Scale-Space Theory in Computer Vision: Proceedings of the First International Conference, Scale-Space'97, Utrecht, The Netherlands*, volume 1252 of *Lecture Notes in Computer Science*. Springer-Verlag, Berlin, July 1997.

[31] R. D. Henkel. Segmentation in scale space. In *Computer Analysis of Images and Patterns. Lecture Notes in Computer Science, vol. 970. Springer-Verlag, pages 41-48*, 1995.

[32] P.T. Jackway. Gradient watersheds in morphological scale-space. *IEEE Transactions on Image Processing*, 5(6):913–921, 1996.

[33] P. Johansen. On the classification of toppoints in scale space. *Mathematical Imaging and Vision*, 4(1):57–67, 1994.

[34] P. Johansen. Local analysis of image scale space. In *Sporring et al. [62]*, pages 139–146, 1997.

[35] P. Johansen, M. Nielsen, and O.F. Olsen. Branch points in one-dimensional Gaussian scale space. *Journal of Mathematical Imaging and Vision*, 13:193–203, 2000.

[36] P. Johansen, S. Skelboe, K. Grue, and J. D. Andersen. Representing signals by their toppoints in scale space. In *Proceedings of the International Conference on Image Analysis and Pattern Recognition (Paris, France, October 1986)*, pages 215–217. IEEE Computer Society Press, 1986.

[37] S. Kalitzin. Topological numbers and singularities. In *Sporring et al. [62]*, pages 181–190, 1997.

[38] S. N. Kalitzin, B. M. ter Haar Romeny, A. H. Salden, P. F. M. Nacken, and M. A. Viergever. Topological numbers and singularities in scalar images. Scale-space evolution properties. *Journal of Mathematical Imaging and Vision*, 9(3):253–296, November 1998.

[39] M. Kerckhove, editor. *Scale-Space and Morphology in Computer Vision*, volume 2106 of *Lecture Notes in Computer Science*. Springer -Verlag, Berlin Heidelberg, 2001.

[40] J. J. Koenderink. The structure of images. *Biological Cybernetics*, 50:363–370, 1984.

[41] J. J. Koenderink. A hitherto unnoticed singularity of scale-space. *IEEE Transactions on Pattern Analysis and Machine Intelligence*, 11(11):1222–1224, 1989.

[42] A. Koster. *Linking Models for Multiscale Image Segmentation.* PhD thesis, Utrecht University, 1995.

[43] A. Kuijper and L.M.J. Florack. Calculations on critical points under gaussian blurring. In *Nielsen et al. [54]*, pages 318–329, 1999.

[44] A. Kuijper and L.M.J. Florack. Hierarchical pre-segmentation without prior knowledge. In *Proceedings of the 8th International Conference on Computer Vision (Vancouver, Canada, July 9–12, 2001)*, pages 487–493, 2001.

[45] A. Kuijper, L.M.J. Florack, and M.A. Viergever. Scale space hierarchy. Technical Report UU-CS-2001-19, Department of Computer Science, Utrecht University, 2001.

[46] A. Kuijper, L.M.J. Florack, and M.A. Viergever. Scale space hierarchy, 2001. submitted.

[47] L. M. Lifshitz and S. M. Pizer. A multiresolution hierarchical approach to image segmentation based on intensity extrema. *IEEE Transactions on Pattern Analysis and Machine Intelligence*, 12(6):529–540, 1990.

[48] T. Lindeberg. Scale–space behaviour of local extrema and blobs. *Journal of Mathematical Imaging and Vision*, 1(1):65–99, 1992.

[49] T. Lindeberg. Detecting salient blob-like image structures and their scales with a scale-space primal sketch: a method for focus-of-attention. *International Journal of Computer Vision*, 11(3):283–318, 1993.

[50] T. Lindeberg. *Scale-Space Theory in Computer Vision.* The Kluwer International Series in Engineering and Computer Science. Kluwer Academic Publishers, 1994.

[51] M. Loog, J.J. Duistermaat, and L.M.J. Florack. On the behavior of spatial critical points under Gaussian blurring. a folklore theorem and scale-space constraints. In *Kerckhove [39]*, pages 183–192, 2001.

[52] Y.-C. Lu. *Singularity Theory and an Introduction to Catastrophe Theory.* Springer-Verlag, Berlin, second corrected printing edition, 1976.

[53] E. Nakamura and N. Kehtarnavaz. Determining number of clusters and prototype locations via multi-scale clustering. *Pattern Recognition Letters*, 19(14):1265–1283, 1998.

[54] M. Nielsen, P. Johansen, O. Fogh Olsen, and J. Weickert, editors. *Scale-Space Theories in Computer Vision*, volume 1682 of *Lecture Notes in Computer Science.* Springer -Verlag, Berlin Heidelberg, 1999.

[55] O. Fogh Olsen. Multi-scale watershed segmentation. In *Sporring et al. [62]*, pages 191–200, 1997.

[56] O. Fogh Olsen. *Generic Image Structure*. PhD thesis, University of Copenhagen, Denmark, 2000.

[57] O. Fogh Olsen and M. Nielsen. Multi-scale gradient magnitude watershed segmentation. In *ICIAP'97 - 9th International Conference on Image Analysis and Processing, volume 1310 of Lecture Notes in Computer Science*, pages 6–13, September 1997.

[58] P. Perona and J. Malik. Scale space and edge detection using anisotropic diffusion. *IEEE Transactions on Pattern Analysis and Machine Intelligence*, 12(7):629–639, 1990.

[59] T. Poston and I. N. Stewart. *Catastrophe Theory and its Applications*. Pitman, London, 1978.

[60] A. H. Salden. *Dynamic Scale-Space Paradigms*. PhD thesis, Utrecht University, 1996.

[61] A. Simmons, S.R. Arridge, P.S. Tofts, and G.J. Barker. Application of the extremum stack to neurological MRI. *IEEE Transactions on Medical Imaging*, 17(3):371–382, June 1998.

[62] J. Sporring, M. Nielsen, L.M.J. Florack, and P. Johansen, editors. *Gaussian Scale-Space Theory*, volume 8 of *Computational Imaging and Vision Series*. Kluwer Academic Publishers, Dordrecht, second edition, 1997.

[63] R. Thom. *Stabilité Structurelle et Morphogénèse*. Benjamin, New york, 1972.

[64] R. Thom. *Structural Stability and Morphogenesis*. Benjamin-Addison Wesley, 1975. translated by D. H. Fowler.

[65] K. Vincken. *Probabilistic Multiscale Image Segmentation by the Hyperstack*. PhD thesis, Utrecht University, 1995.

[66] K.L. Vincken, A.S.E. Koster, and M.A. Viergever. Probabilistic multiscale image segmentation. *IEEE Transactions on Pattern Analysis and Machine Intelligence*, 19(2):109–120, 1997.

[67] T. Wada and M. Sato. Scale-space tree and its hierarchy. In *ICPR90*, volume II, pages 103–108, 1990.

[68] J. Weickert. *Anisotropic Diffusion in Image Processing*. Teubner, Stuttgart, 1998.

[69] A.P. Witkin. Scale-space filtering. In *Proceedings of the Eighth International Joint Conference on Artificial Intelligence*, pages 1019–1022, 1983.

[70] E.C. Zeeman. *Catastrophe Theory: Selected Papers, 1972-1977*. Addison-Wesley Publishing Company, 1977.